

Graphene may help to solve the Casimir conundrum in indium tin oxide systems

G. L. Klimchitskaya^{1,2} and V. M. Mostepanenko^{1,2,3}

¹*Central Astronomical Observatory at Pulkovo of the Russian Academy of Sciences, Saint Petersburg, 196140, Russia*

²*Institute of Physics, Nanotechnology and Telecommunications, Peter the Great Saint Petersburg Polytechnic University, Saint Petersburg, 195251, Russia*

³*Kazan Federal University, Kazan, 420008, Russia*

Abstract

We reconsider the long-explored problem that the magnitude of the measured Casimir force between an Au sphere and an indium tin oxide (ITO) film decreases significantly with no respective changes in the ITO dielectric permittivity required by the Lifshitz theory. Two plausible resolutions of this conundrum are discussed: the phase transition of an ITO film from metallic to dielectric state and the modification of a film surface under the action of UV light. To exclude the latter option, we propose an improvement in the experimental scheme by adding a graphene sheet on top of an ITO film. The formalism is developed allowing precise calculation of the Casimir force between an Au sphere and a graphene sheet on top of ITO film deposited on a quartz substrate. In doing so Au, ITO, and quartz are described by the frequency-dependent dielectric permittivities and real graphene sheet with nonzero mass-gap parameter and chemical potential by the polarization tensor at nonzero temperature. Numerical computations performed both before and after the phase transition resulting from the UV treatment show that the presence of graphene leads to only a minor decrease in the drop of the Casimir force which remains quite measurable. At the same time, in the presence of graphene the guess that an observed drop originates from the modification of an ITO surface by the UV light breaks down. Similar results are obtained for the configuration of two parallel plates consisting of a graphene sheet, an ITO film and a quartz substrate. The proposed experiments involving additional graphene sheets may help in resolution of the problems arising in application of the Lifshitz theory to real materials.

I. INTRODUCTION

With advances in microelectronics, the fluctuation-induced van der Waals and Casimir forces attract the particular attention of many researches. Taking into account that these forces become dominant at separations below a few hundred nanometers, they can be used for actuation of various microdevices in place of the electric force [1, 2]. Work in this scientific direction has already come up with many promising results. Thus, the stability of Casimir-actuated microdevices depending on geometry and dielectric properties of materials was considered in Refs. [3, 4]. The role of surface roughness in the actuation of microelectromechanical systems by the Casimir force was found [5, 6]. Sensitivity of micromechanical Casimir actuation on amorphous-to-metallic phase transitions was also determined [7]. Much attention is given to recent experimental demonstration of the Casimir forces on a silicon micromechanical chip [8, 9]. Moreover, there are suggestions to control mechanical switchers using the Casimir force between a graphene sheet and a silicon membrane [10] and to devise an optical chopper driven by the Casimir force [11].

The wide diversity of promising practical implementations of fluctuation-induced forces in various microdevices makes highly desirable a clear knowledge of their nature. The unified theoretical description of the van der Waals and Casimir forces is given by the fundamental Lifshitz theory [12, 13], which expresses both the free energy and force via the frequency-dependent dielectric permittivity of boundary materials. It happened, however, in some cases that a comparison between the experimental data and theoretical predictions resulted in big surprises.

A serious conundrum was revealed in application of the Lifshitz theory to systems including indium tin oxide (ITO) films. This semiconductor finds wide applications as an optoelectronic material possessing high electrical conductivity and optical transparency, but it is opaque in the ultraviolet (UV) frequency region. Thin ITO films can be easily deposited on different substrates [14]. Pioneer measurements of the Casimir interaction between an Au sphere and an ITO film have been performed in Refs. [15, 16]. The gradient of the Casimir force was measured to be roughly 40%–50% smaller than that between an Au sphere and an Au plate. This result is in qualitative agreement with theoretical predictions of the Lifshitz theory.

A short time later the Casimir force between an Au-coated polystyrene sphere and quartz

substrate coated with an ITO film was measured in Refs. [17, 18]. The distinctive property of this experiment is that, after the force measurements were completed, the ITO sample was UV-treated for 12 h, and then the force measurements were again performed. Quite unexpectedly, the measured Casimir force for the UV-treated samples turned out to be for 21% and 35% smaller in magnitude at 60 and 130 nm sphere-plate separations, respectively, than for the untreated ones. The observed decrease was not associated with respective modifications of the optical properties of ITO under the influence of UV treatment. This was confirmed by means of ellipsometry measurements performed for both untreated and UV-treated ITO samples. As a consequence, an immediate application of the Lifshitz theory has led to almost coinciding Casimir forces for the untreated and UV-treated ITO samples in clear contradiction with the experimental evidence.

The hypothetical explanation of the revealed contradiction was provided in Refs. [17, 18]. It was anticipated that the UV treatment causes the phase transition of the ITO film from metallic to dielectric state. If, in addition, one assumes that, when calculating the Casimir force, the contribution of free charge carriers to the ITO dielectric permittivity should be taken into account in the metallic state, but should be disregarded in the dielectric state, the theoretical results turn out to be in good agreement with the measurement data. The latter assumption is somewhat foreign in the formalism of the Lifshitz theory, but it was already successfully used for interpretation of several earlier experiments. Thus, it was found that the measured difference in the Casimir forces between an Au sphere and a Si plate in the absence and in the presence of laser pulse, transforming it from the dielectric to metallic state, agree with theoretical predictions of the Lifshitz theory only if free charge carriers in the dielectric Si are disregarded [19, 20]. If free charge carriers in the dielectric Si are taken into account, the theoretical predictions are excluded by the data. One further example is given by the experiment on measuring the thermal Casimir-Polder force between ^{87}Rb atoms and a SiO_2 plate [21]. Here, again, the Lifshitz theory was found to be in agreement with the measurement data if the free charge carriers in the dielectric plate are disregarded [21, 22], but the same theory was excluded by the data if the free charge carriers are taken into account in computations [22]. It was shown also that inclusion of free charge carriers in calculation of the Casimir entropy for dielectric materials results in violation of the Nernst heat theorem, which is satisfied if the free charge carriers are disregarded [23–26].

This raises the question of whether an ITO film really undergoes the phase transition

under the influence of UV treatment or a decrease in magnitude of the Casimir force for the UV-treated film is due to reducing of some foreign insertions like dust and contaminants by the action of UV light. The former is supported by the observation that the UV treatment of ITO leads to a lower mobility of charge carriers [27], whereas the latter is based on the fact that the UV light is often used for cleaning of surfaces [28], as well as some other agents (for instance, the Ar-ion cleaning of Au surfaces was recently used in measurements of the Casimir force [29]). For the resolution of the above conundrum, it is necessary to assess what is the real impact of UV light on an ITO film.

In this paper, we propose a minor modification of experiments described in Res. [17, 18] which allows definite conclusions concerning the role of UV treatment of an ITO test body. It is suggested to add a graphene sheet on top of an ITO film. The Casimir force in graphene systems is a subject of considerable theoretical study using different calculation approaches (see, e.g., Refs. [30–34]). It was calculated on the basis of first principles of quantum electrodynamics at nonzero temperature using the polarization tensor of graphene in (2+1)-dimensional space-time [35–43]. The theoretical results were found to be in good agreement [44] with measurements of the gradient of the Casimir force between an Au-coated sphere and a graphene-coated substrate [45]. Our proposal is based on the fact that graphene sheets are almost transparent for the UV region [46]. Thus, the presence of a graphene sheet would leave intact an assumption that ITO undergoes the phase transition under the influence of UV light, but make improbable a guess that the observed decrease in the magnitude of the Casimir force for the UV-treated sample is due to the effect of cleaning.

To confirm the feasibility of the proposed experiment, we calculate the Casimir force between an Au-coated sphere and a graphene sheet on top of an ITO film coating the quartz substrate both before and after the UV treatment. Computations are made using the same values of all parameters as in the experiments of Refs. [17, 18]. In so doing, the free charge carriers in the untreated (metallic) ITO are taken into account and in the UV-treated either taken into account or disregarded. It is shown that in the presence of graphene the Casimir force for the UV-treated samples would be from 20% to 30% smaller in magnitude when separation varies from 60 to 150 nm if the free charge carriers are disregarded. This makes experiment with an additional graphene sheet quite feasible. We have also computed the Casimir pressure between two ITO films deposited on two parallel quartz plates both before and after the UV treatment. Similar to the case of sphere-plate geometry, it was assumed

that the UV treatment results in a phase transition of ITO from the metallic to dielectric state. According to our computational results, under an assumption of the phase transition, the Casimir pressure is changed by the UV light from 56% to 65% when separation varies from 150 to 300 nm. If an additional graphene sheet is added on each plate, this change varies from 47% to 52%, i.e., remains easily observable.

The paper is organized as follows. In Sec. II the general formalism for the UV treated and untreated ITO films is presented in sphere-plate geometry in the presence of an additional graphene sheet. Section III reports the results of numerical computations for the impact of graphene sheet on the Casimir force in sphere-plate geometry. In Sec. IV similar results are obtained for the Casimir pressure between two ITO plates coated with graphene. In Sec. V the reader will find our conclusions and discussion.

II. THE CASIMIR FORCE IN UV-TREATED AND UNTREATED INDIUM TIN OXIDE SYSTEM IN THE PRESENCE OF GRAPHENE

We consider the configuration of a sphere above a plate. In Refs. [17, 18] the radius of an Au-coated sphere was $R = 101.2 \mu\text{m}$. The thickness of an Au coating was sufficiently large to consider sphere as all-gold. The sphere-plate separation a exceeds 60 nm. For generality from the very beginning we consider the plate as a layer structure consisting of a graphene sheet, an ITO film $\text{In}_2\text{O}_3\text{:Sn}$ of thickness $d = 74.6 \text{ nm}$, and a quartz substrate of 1 mm thickness. With respect to measurements of the Casimir force, the latter can be considered as a semispace.

The Casimir force F_C as a function of a at temperature T is given by the Lifshitz theory where the responses of gold, ITO and quartz to electromagnetic fluctuations are described by the frequency-dependent dielectric permittivities and the response of graphene — by the polarization tensor in (2+1)-dimensional space-time. In the framework of the proximity force approximation, which is accurate up to a fraction of a percent for the above parameters [47–50], the Lifshitz formula for the layered structure has the usual form

$$F_C(a, T) = k_B T R \sum_{l=0}^{\infty}{}' \int_0^{\infty} k_{\perp} dk_{\perp} \times \sum_{\alpha} \ln \left[1 - R_{\alpha}^{(p)}(i\xi_l, k_{\perp}) r_{\alpha}^{(0,3)}(i\xi_l, k_{\perp}) e^{-2q_l a} \right], \quad (1)$$

where k_B is the Boltzmann constant, $\xi_l = 2\pi k_B T l / \hbar$ with $l = 0, 1, 2, \dots$ are the Matsubara frequencies, k_\perp is the magnitude of the project of the wave vector on the plane of graphene, the prime on the summation sign multiplies the term with $l = 0$ by $1/2$, and

$$q_l = \left(k_\perp^2 + \frac{\xi_l^2}{c^2} \right)^{1/2}. \quad (2)$$

The summation in α in Eq. (1) is by two independent polarizations of the electromagnetic field, transverse magnetic ($\alpha = \text{TM}$) and transverse electric ($\alpha = \text{TE}$). In line with this the TM and TE reflection coefficients of the layered plate are given by [45]

$$R_\alpha^{(p)}(i\xi_l, k_\perp) = \frac{r_\alpha^{(g)} + r_\alpha^{(u)} \left(1 \mp 2r_\alpha^{(g)} \right)}{1 - r_\alpha^{(g)} r_\alpha^{(u)}}, \quad (3)$$

where the signs minus and plus are for $\alpha = \text{TM}$ and TE , respectively. Here, the reflection coefficients $r_\alpha^{(u)}$ are on a two-layered structure underlying the graphene sheet, i.e., on an ITO film of thickness d and a thick quartz substrate. It is given by

$$r_\alpha^{(u)}(i\xi_l, k_\perp) = \frac{r_\alpha^{(0,1)} + r_\alpha^{(1,2)} e^{-2k_l^{(1)} d}}{1 + r_\alpha^{(0,1)} r_\alpha^{(1,2)} e^{-2k_l^{(1)} d}}, \quad (4)$$

where the dielectric permittivities of ITO and quartz at the imaginary Matsubara frequencies are notated as $\varepsilon_l^{(1)} = \varepsilon^{(1)}(i\xi_l)$ and $\varepsilon_l^{(2)} = \varepsilon^{(2)}(i\xi_l)$, respectively,

$$k_l^{(n)} = \left[k_\perp^2 + \varepsilon_l^{(n)} \frac{\xi_l^2}{c^2} \right]^{1/2}, \quad (5)$$

and

$$\begin{aligned} r_{\text{TM}}^{(n,n')}(i\xi_l, k_\perp) &= \frac{\varepsilon_l^{(n')} k_l^{(n)} - \varepsilon_l^{(n)} k_l^{(n')}}{\varepsilon_l^{(n')} k_l^{(n)} + \varepsilon_l^{(n)} k_l^{(n')}}, \\ r_{\text{TE}}^{(n,n')}(i\xi_l, k_\perp) &= \frac{k_l^{(n)} - k_l^{(n')}}{k_l^{(n)} + k_l^{(n')}}. \end{aligned} \quad (6)$$

Note that for $n = 0$ we have the vacuum gap $\varepsilon_l^{(0)} = 1$. The reflection coefficient $r_\alpha^{(0,3)}$ in Eq. (1) is also given by Eq. (6) with $n = 0$ and $n' = 3$ where $\varepsilon_l^{(3)} = \varepsilon^{(3)}(i\xi_l)$ are the values of the dielectric permittivity of Au at the pure imaginary Matsubara frequencies.

The reflection coefficients $r_\alpha^{(g)}$ on a graphene sheet in Eq. (3) still remain to be defined. They are expressed via the polarization tensor of graphene in the following way [35, 42]

$$\begin{aligned} r_{\text{TM}}^{(g)}(i\xi_l, k_\perp) &= \frac{q_l \Pi_{00,l}}{q_l \Pi_{00,l} + 2\hbar k_\perp^2}, \\ r_{\text{TE}}^{(g)}(i\xi_l, k_\perp) &= -\frac{\Pi_l}{\Pi_l + 2\hbar k_\perp^2 q_l}. \end{aligned} \quad (7)$$

The quantities $\Pi_{00,l}$ and $\Pi_{\text{tr},l} = \Pi_{\beta,l}^\beta$ are the 00 component and the trace of the polarization tensor of graphene, calculated at the pure imaginary Matsubara frequencies,

$$\Pi_l = k_\perp^2 \Pi_{\text{tr},l} - q_l^2 \Pi_{00,l} \quad (8)$$

and q_l is defined in Eq. (2).

It is convenient to present the explicit expressions separately for $\Pi_{00,0}$, Π_0 and for $\Pi_{00,l}$, Π_l with $l \geq 1$. Thus, for $l = 0$ one obtains [42]

$$\begin{aligned} \Pi_{00,0}(k_\perp) &= \alpha \hbar c \frac{k_\perp}{v_F} \Psi\left(\frac{\Delta}{\hbar v_F k_\perp}\right) + \frac{8\alpha k_B T c}{v_F^2} \ln \left[\left(e^{\frac{\mu}{k_B T}} + e^{-\frac{\Delta}{2k_B T}} \right) \left(e^{-\frac{\mu}{k_B T}} + e^{-\frac{\Delta}{2k_B T}} \right) \right] \\ &\quad - \frac{4\alpha \hbar c k_\perp}{v_F} \int_{D_0}^{\sqrt{1+D_0^2}} du \left(\frac{1}{e^{B_l u + \frac{\mu}{k_B T}} + 1} + \frac{1}{e^{B_l u - \frac{\mu}{k_B T}} + 1} \right) \frac{1 - u^2}{\sqrt{1 - u^2 + D_0^2}}, \\ \Pi_0(k_\perp) &= \alpha \hbar \frac{v_F k_\perp^3}{c} \Psi\left(\frac{\Delta}{\hbar v_F k_\perp}\right) \\ &\quad + 4\alpha \hbar \frac{v_F k_\perp^3}{c} \int_{D_0}^{\sqrt{1+D_0^2}} du \left(\frac{1}{e^{B_l u + \frac{\mu}{k_B T}} + 1} + \frac{1}{e^{B_l u - \frac{\mu}{k_B T}} + 1} \right) \frac{-u^2 + D_0^2}{\sqrt{1 - u^2 + D_0^2}}, \end{aligned} \quad (9)$$

Here, $\alpha = e^2/(\hbar c)$ is the fine structure constant, $v_F \approx c/300$ is the Fermi velocity of the quasiparticles in graphene, Δ is the mass-gap parameter, which is usually not equal to zero, especially for graphene deposited on a substrate [51–53], μ is the chemical potential describing the fraction of extraneous atoms, which are always present in graphene [54], and the following notations are introduced:

$$\begin{aligned} \Psi(x) &= 2 \left[x + (1 - x^2) \arctan \frac{1}{x} \right], \\ D_0 &= \frac{\Delta}{\hbar v_F k_\perp}, \quad B_0 = \frac{\hbar v_F k_\perp}{2k_B T}. \end{aligned} \quad (10)$$

For $l \geq 1$ the exact expressions for $\Pi_{00,l}$ and Π_l are somewhat more complicated. However, at $T = 300$ K at sufficiently large separations ($a > 60$ nm, as in Refs. [17, 18]) the following approximate expressions lead to the same results as the exact ones up to a small fraction of a percent:

$$\begin{aligned} \Pi_{00,l}(k_\perp) &\approx \alpha \hbar \frac{c k_\perp^2}{\xi_l} \left[\Psi\left(\frac{\Delta}{\hbar \xi_l}\right) + \tilde{Y}_l(T, \Delta, \mu) \right], \\ \Pi_l(k_\perp) &\approx \alpha \hbar \frac{\xi_l k_\perp^2}{c} \left[\Psi\left(\frac{\Delta}{\hbar \xi_l}\right) + \tilde{Y}_l(T, \Delta, \mu) \right], \end{aligned} \quad (11)$$

where

$$\begin{aligned} \tilde{Y}_l(T, \Delta, \mu) = & 2 \int_{\Delta/(\hbar\xi_l)}^{\infty} du \left(\frac{1}{e^{B_l u + \frac{\mu}{k_B T}} + 1} + \frac{1}{e^{B_l u - \frac{\mu}{k_B T}} + 1} \right) \\ & \times \frac{u^2 + \left(\frac{\Delta}{\hbar\xi_l}\right)^2}{u^2 + 1} \end{aligned} \quad (12)$$

and

$$B_l = \frac{\hbar c \tilde{q}_l}{2k_B T}, \quad \tilde{q}_l = \sqrt{\frac{v_F^2}{c^2} k_{\perp}^2 + \frac{\xi_l^2}{c^2}}. \quad (13)$$

If one puts $r_{\alpha}^{(g)} = 0$ in Eq. (3), this leads to $R_{\alpha}^{(p)} = r_{\alpha}^{(u)}$, where $r_{\alpha}^{(u)}$ is defined in Eq. (5), and Eq. (1) returns us back to the Casimir force between an Au sphere and a quartz substrate coated with an ITO film, as in the experiment of Refs. [17, 18].

As was mentioned in Sec. I, measurements of the Casimir force in Refs. [17, 18] have been performed for both untreated and UV-treated ITO samples. The UV treatment was performed by means of a mercury lamp with the primary peak at the wavelength 254 nm. The imaginary parts of the dielectric permittivities were obtained from ellipsometry measurements performed both before and after UV treatment. Only minor differences in these imaginary parts were observed for the untreated and UV-treated samples. In Fig. 1 we show the dielectric permittivity of ITO as a function of the imaginary frequency found with the help of Kramers-Kronig relations (see Refs. [17, 18] for details). The solid lines 1 and 2 demonstrate the dielectric permittivity before the UV treatment with account of free charge carriers and after the UV treatment without account of free charge carriers, respectively. The dashed line shows the dielectric permittivity after the UV treatment, but with included free charge carriers. The dielectric permittivities of Au and quartz along the imaginary frequency axis were obtained using the tabulated optical data [55] and the averaged analytic representation [56] (see Refs. [17, 18] for details).

The above formalism (with $r_{\alpha}^{(g)} = 0$) leads to two theoretical bands for the Casimir force F_C between an Au sphere and untreated and UV-treated ITO film deposited on a quartz substrate shown in Fig. 2. The bottom band is computed at $T = 300$ K for an untreated film using the solid line 1 in Fig. 1, i.e., assuming that ITO is in a metallic state. The top band is computed at the same temperature for a UV-treated film using the solid line 2 in Fig. 1 under an assumption that the UV treatment caused the phase transition from metallic to dielectric state. Note that the surface roughness measured by means of an atomic force microscope was taken into account using the geometrical averaging [18]. It contributes

2.2% of the force at $a = 60$ nm and less than 1% at $a \geq 90$ nm. The widths of the bands are determined by the theoretical uncertainties mostly connected with the necessity to extrapolate the ellipsometry data to outside the regions where they are taken. The mean measured Casimir forces for the untreated and UV-treated samples are shown together with their experimental errors determined at a 95% confidence level by the bottom and top sets of crosses, respectively [17, 18]. As is seen in Fig. 2, the theory assuming phase transition as a result of UV treatment is in a very good agreement with the data. If after the UV treatment the dielectric permittivity given by the dashed line in Fig. 1 is used in calculations, the obtained theoretical results almost coincide with the bottom line in Fig. 2, i.e., would be in serious contradiction with the measurement data given by the top set of crosses.

In Fig. 2 it is seen that separation between the two bands exceeds significantly both the experimental and theoretical errors. In the next section we show that adding a graphene sheet on top of ITO, which prevents the surface of ITO from being modified by the UV light, leaves the theoretical predictions before and after UV treatment considerably different.

III. IMPACT OF GRAPHENE ON THE CASIMIR FORCE IN SPHERE-PLATE GEOMETRY

Now we assume that there is a graphene sheet on top of ITO film. In this case the Casimir force between an Au sphere and a layered plate consisting of graphene, ITO and quartz substrate is given by Eqs. (1)–(13). At first, we find what is the qualitative impact of graphene sheet on the theoretical bands shown in Fig. 2. This will be done for a pristine graphene with $\Delta = \mu = 0$. Then we will determine the impact of the mass-gap parameter Δ and chemical potential μ .

The computational results for the Casimir force F_C in the presence of a graphene sheet with $\Delta = \mu = 0$ on an ITO film are shown in Fig. 3(a) by the bottom and top dark bands as functions of separation for the untreated and UV-treated samples, respectively. In the same figure the gray bands reproduce that ones computed in the original experimental configuration of Refs. [17, 18], i.e., in the absence of a graphene sheet. As in Fig. 2, the bottom band is computed using the dielectric permittivity of ITO with account of free charge carriers (the solid line 1 in Fig. 1) and the top band is computed with free charge carriers disregarded (the solid line 2 in Fig. 1). As can be seen in Fig. 3(a), the presence of a graphene

sheet increases the force magnitudes for a UV-treated sample, but leaves them almost intact for an untreated one. Computations show that for an untreated sample the presence of a graphene sheet increases the force magnitude by approximately 1%. This cannot be noticed in the figure. Note also that the width of the bands is determined by the uncertainties in the dielectric permittivity of ITO. The same widths are obtained for a graphene sheet with nonzero mass-gap parameter $\Delta \leq 0.1$ eV and chemical potential $\mu \leq 0.5$ eV.

As an illustration, Fig. 3(b) shows the mean lines of the bands. The bottom (dark) line almost coincides with the gray one. This shows that for an untreated (metallic) sample graphene makes only a minor impact on the Casimir force. At the same time, the medium (dark) line is well away from the top (gray) line, i.e., an impact of graphene on the UV-treated (dielectric) sample is quite sensible. As an example, in the presence of graphene the drop in the magnitude of the Casimir force due to UV treatment varies from 20% to 35% when separation varies from 60 to 150 nm. An inset in Fig. 3(b) shows the differences δF_C between the Casimir forces $F_C^{(g)}$ for UV-treated and untreated ITO films coated with graphene (the solid line) and the Casimir forces F_C for uncoated UV-treated and untreated ITO films (the dashed line). As is seen in the inset, the presence of graphene coating leads to only a minor decrease in the effect of UV treatment.

The main problem for the feasibility of the proposed experiment is how large is the force difference between the lower border of the top dark band (for a UV-treated sample) and the upper border of the bottom dark band (for an untreated sample) in Fig. 3(a), as compared to the experimental errors. For the resolution of this problem in the case of real graphene sheets with nonzero Δ and μ , we investigate the quantity

$$F_C^{\text{diff}}(a, \mu) = \min [F_C^{\text{UV}}(a, \mu, \Delta) - F_C(a, \mu, \Delta)] . \quad (14)$$

Here, F_C and F_C^{UV} are the Casimir forces for the untreated and UV-treated samples and the minimum value is taken over the uncertainties in the dielectric permittivity of ITO and unknown value of the mass-gap parameter of a graphene sheet in the limits from 0 to 0.1 eV.

In Fig. 4 we present the computational results for the quantity F_C^{diff} by the four lines from top to bottom as the functions of chemical potential of graphene at $T = 300$ K at the separations $a = 60, 80, 100$, and 120 nm, respectively. As is seen in Fig. 4, there is an almost linear dependence of F_C^{diff} on μ at $a = 60$ nm which becomes weaker and weaker with increasing separation. Thus, at $a = 60, 80, 100$, and 120 nm we have $F_C^{\text{diff}} = 42.1, 25.8, 16.9$,

and 11.7 pN for $\mu = 0$, respectively, and $F_C^{\text{diff}} = 37.9, 23.8, 15.8$, and 11.1 pN for $\mu = 0.5$ eV at the same respective separation distances.

The obtained results should be compared with the experimental error in measurement of the quantity F_C^{diff} which is equal to the sum of errors in measurements of F_C and F_C^{UV} . According to the results of Refs. [17, 18], at separations of 60, 80, 100, and 120 nm the error in F_C^{diff} determined at a 95% confidence level is equal to 5.5, 4.5, 4.0, and 3.5 pN, respectively. Thus, in spite of the fact that the presence of a graphene sheet somewhat decreases the differences in theoretical predictions for the Casimir force between an Au sphere and the untreated and UV-treated ITO films, the feasibility of the proposed experiment is confirmed.

IV. IMPACT OF GRAPHENE ON THE CASIMIR PRESSURE BETWEEN TWO INDIUM TIN OXIDE PLATES

Taking into consideration that with recent development of chip technologies [8, 9] the precise Casimir measurements in plane-parallel geometries become quite realizable, we consider here one more modification of the proposed experiment gaining an advantage from using two ITO films. For this purpose we consider the configuration of two parallel plates each of which consists of a graphene sheet, an ITO film of thickness d , and a quartz substrate. In so doing the graphene sheets facing each other are separated by the distance a . The Casimir pressure in this configuration is given by the Lifshitz formula [12, 13]

$$P_C(a, T) = -\frac{k_B T}{\pi} \sum_{l=0}^{\infty}{}' \int_0^{\infty} q_l k_{\perp} dk_{\perp} \times \sum_{\alpha} \left[\frac{e^{2q_l a}}{R_{\alpha}^{(p)2}(i\xi_l, k_{\perp})} - 1 \right]^{-1}, \quad (15)$$

where all necessary notations are introduced in Sec. II.

First we consider what is the effect of UV treatment for two parallel ITO films deposited on quartz substrate in the absence of graphene sheets (i.e., for $r_{\alpha}^{(g)} = 0$ in all equations). In Fig. 5(a) the mean values of the Casimir pressure computed at $T = 300$ K are plotted as functions of separation by the bottom and top lines for the untreated and UV-treated ITO samples, respectively. In the same way as in Sec. III, the bottom line is computed with the dielectric permittivity of ITO shown by the solid line 1 in Fig. 1, and the top line with the dielectric permittivity shown by the solid line 2 in the same figure. If after the

UV treatment the free charge carriers are taken into account (i.e., the dielectric permittivity shown by the dashed line in Fig. 1 is used) the obtained Casimir pressure is again presented to a high accuracy by the bottom line in Fig. 5(a). As is seen in Fig. 5(a), in the absence of graphene the differences in the Casimir pressures between the cases of untreated and UV-treated samples vary from 283.3 to 26.2 mPa when separation increases from 150 to 300 nm. The relative drop in the Casimir pressure due to UV treatment varies from 57% to 65% when separation increases from 150 to 300 nm, respectively. Here we consider larger separation distances than in Sec. III because it is common to determine the Casimir pressure using the dynamic measurement schemes.

Now we assume that there are graphene sheets with $\Delta = \mu = 0$ on top of ITO films and repeat computations of the Casimir pressure (15) where $r_\alpha^{(g)}$ is given by Eq. (7). In Fig. 5(b) computational results are shown as the bottom and top bands where the band widths are caused by the uncertainties in the dielectric permittivity of ITO. The bottom band is for an untreated sample and the top band for a UV-treated one, respectively. As is seen in Fig. 5(b), the presence of graphene sheets decreases the differences in the Casimir pressures in the cases of untreated and UV-treated samples, but to only a small extent. Thus, at separations $a = 150, 200, 250$, and 300 nm the differences between the lower border of the top band and the upper border of the bottom band are equal to 203.0, 78.4, 36.8, and 19.6 mPa, respectively. Note that the nonzero chemical potential of graphene makes only a minor impact on the obtained results. In the presence of graphene, the relative drop in the magnitude of the Casimir pressure due to UV treatment increases from 41% to 49% when separation increases from 150 to 300 nm, respectively.

Since in Sec. III the same thickness d of an ITO film, as in the experiment of Refs. [17, 18] was used, here we consider the dependence of the obtained results on d . For this purpose we calculate the quantity

$$P_C^{\text{diff}}(a, d) = \min [P_C^{\text{UV}}(a, d, \mu, \Delta) - P_C(a, d, \mu, \Delta)]. \quad (16)$$

Here, P_C and P_C^{UV} are the Casimir pressures for untreated and UV-treated samples. The minimum value in Eq. (16) is taken over the uncertainties in the dielectric permittivity of ITO and over possible values of the mass-gap parameter of graphene Δ and its chemical potential μ . Taking into account that with increasing μ the magnitude of the Casimir pressure increases, whereas an increase of Δ leads to the opposite result [42], we put $\mu =$

0.5 eV, $\Delta = 0$ in the computations of P_C^{UV} and $\mu = 0$, $\Delta = 0.1$ eV in the computations of P_C in order to reach the minimum value.

The computational results for P_C^{diff} at $T = 300$ K as functions of the thickness of an ITO film are shown in Fig. 6 by the four lines plotted from top to bottom at separations $a = 150$, 175, 200, and 250 nm between the plates, respectively. As is seen in Fig. 6, the quantity P_C^{diff} increases rather slowly with increasing thickness of an ITO film. This increase becomes more rapid only at the shortest separation considered ($a = 150$ nm). Taking into account that in the dynamic experiments using the atomic force microscope the effective Casimir pressure is measured with an error of 1 mPa [57], an error in the determination of P_C^{diff} could be equal to 2 mPa. It is much smaller than the calculated values of P_C^{diff} shown in Fig. 6 for any thickness of an ITO film. This shows that the proposed experiment using two ITO films coated with graphene sheets is well suited for observation of the drop in the Casimir pressure under an impact of UV treatment.

V. CONCLUSIONS AND DISCUSSION

In this paper, we have reconsidered the Casimir conundrum in indium tin oxide systems consisting in the fact that the measured Casimir force drops in magnitude significantly under the impact of UV treatment with no respective changes in the dielectric permittivity of ITO, as required by the Lifshitz theory. In Refs. [17, 18] this drop, which varies from 21% to 35% depending on separation, was hypothetically explained under an assumption that the UV treatment causes the phase transition of ITO from metallic to dielectric state where the free charge carriers should not be taken into account similar to two other experiments of this kind [19–22]. As an alternative explanation, one could guess that the UV light modifies an ITO surface by making some kind of cleaning and this results in respective changes of the Casimir force.

We have proposed a modification in the experimental scheme of Refs. [17, 18] by adding a graphene sheet on top of ITO film. This sheet is almost transparent to the UV light, but prevents the surface of ITO from being modified. The general formalism for calculation of the Casimir force between an Au sphere and a graphene sheet on top of ITO film deposited on a quartz substrate is developed. In doing so Au, ITO, and quartz are described by the frequency-dependent dielectric permittivities and graphene by the polarization tensor at

nonzero temperature. Numerical computations using this formalism demonstrate that the presence of a graphene sheet with different values of the mass-gap parameter and chemical potential results in only a slight decrease in the drop of the Casimir force magnitude after the UV treatment of an ITO film. This drop far exceeds the experimental error confirming the feasibility of the proposed experiment.

As one more proposal, the configuration of two parallel graphene sheets on top of ITO films deposited on quartz substrates is considered. The Casimir pressures are computed both in the absence and in the presence of graphene sheets before and after the UV treatment. Thus, in the absence of graphene the drop in the Casimir pressure due to UV treatment varies from 57% to 65% depending on separation. In the presence of graphene sheets this drop, although becomes somewhat smaller, as yet exceeds the experimental error by the factor varying from 101 to 10 at different separations between plates. We have also investigated the dependence of the obtained results on the thickness of an ITO film and found that it may vary over a wide range without damage to the proposed experiment.

To conclude, both suggested experiments involving additional graphene layers may be helpful for the resolution of the Casimir conundrum in indium tin oxide systems and for further investigation of other unresolved problems in application of the Lifshitz theory to real materials.

Acknowledgments

The work of V.M.M. was partially supported by the Russian Government Program of Competitive Growth of Kazan Federal University.

-
- [1] H. B. Chan, V. A. Aksyuk, R. N. Kleiman, D. J. Bishop, and F. Capasso, Quantum mechanical actuation of microelectromechanical system by the Casimir effect, *Science* **291**, 1941 (2001).
 - [2] H. B. Chan, V. A. Aksyuk, R. N. Kleiman, D. J. Bishop, and F. Capasso, Nonlinear micromechanical Casimir oscillator, *Phys. Rev. Lett.* **87**, 211801 (2001).
 - [3] J. Barcenas, L. Reyes, and R. Esquivel-Sirvent, Scaling of micro- and nanodevices actuated by the Casimir force, *Appl. Phys. Lett.* **87**, 263106 (2005).

- [4] R. Esquivel-Sirvent and R. Pérez-Pascual, Geometry and charge carrier induced stability in Casimir actuated nanodevices, *Eur. Phys. J. B* **86**, 467 (2013).
- [5] W. Broer, G. Palasantzas, J. Knoester, and V. B. Svetovoy, Significance of the Casimir force and surface roughness for actuation dynamics of MEMS, *Phys. Rev. B* **87**, 125413 (2013).
- [6] W. Broer, H. Waalkens, V. B. Svetovoy, J. Knoester, and G. Palasantzas, Nonlinear actuation dynamics of driven Casimir oscillators with rough surfaces, *Phys. Rev. Applied* **4**, 054016 (2015).
- [7] M. Sedighi, W. Broer, G. Palasantzas, and B. J. Kooi, Sensitivity of micromechanical actuation on amorphous to crystalline phase transformations under the influence of Casimir forces, *Phys. Rev. B* **88**, 165423 (2013).
- [8] J. Zou, Z. Marcet, A. W. Rodriguez, M. T. H. Reid, A. P. McCauley, I. I. Kravchenko, T. Lu, Y. Bao, S. G. Johnson, and H. B. Chan, Casimir forces on a silicon micromechanical chip, *Nature Commun.* **4**, 1845 (2013).
- [9] L. Tang, M. Wang, C. Y. Ng, M. Nolic, C. T. Chan, A. W. Rodriguez, and H. B. Chan, Measurement of non-monotonic Casimir forces between silicon nanostructures, *Nature Photonics* **11**, 97 (2017).
- [10] N. Inui, Optical switching of a graphene mechanical switch using the Casimir effect, *J. Appl. Phys.* **122**, 104501 (2017).
- [11] G. L. Klimchitskaya, V. M. Mostepanenko, V. M. Petrov, and T. Tschudi, Optical chopper driven by the Casimir force, *Phys. Rev. Applied* **10**, 014010 (2018).
- [12] E. M. Lifshitz and L. P. Pitaevskii, *Statistical Physics*, Pt II (Pergamon Press, Oxford, 1984)
- [13] M. Bordag, G. L. Klimchitskaya, U. Mohideen, and V. M. Mostepanenko, *Advances in the Casimir Effect* (Oxford University Press, Oxford, 2015).
- [14] H. L. Hartnagel, A. L. Dawar, A. K. Jain, and C. Jagadish, *Semiconducting Transparent Thin Films* (Institute of Physics Publishing, Bristol, 1995).
- [15] S. de Man, K. Heeck, R. J. Wijngaarden, and D. Iannuzzi, Halving the Casimir force with conductive oxides, *Phys. Rev. Lett.* **103**, 040402 (2009).
- [16] S. de Man, K. Heeck and D. Iannuzzi, Halving the Casimir force with conductive oxides: Experimental details, *Phys. Rev. A* **82**, 062512 (2010).
- [17] C.-C. Chang, A. A. Banishev, G. L. Klimchitskaya, V. M. Mostepanenko, and U. Mohideen, Reduction of the Casimir force from indium tin oxide film by UV treatment, *Phys. Rev. Lett.*

- 107**, 090403 (2011).
- [18] A. A. Banishev, C.-C. Chang, R. Castillo-Garza, G. L. Klimchitskaya, V. M. Mostepanenko, and U. Mohideen, Modifying the Casimir force between indium tin oxide plate and Au sphere, *Phys. Rev. B* **85**, 045436 (2012).
 - [19] F. Chen, G. L. Klimchitskaya, V. M. Mostepanenko, and U. Mohideen, Demonstration of optically modulated dispersion forces, *Opt. Express* **15**, 4823 (2007).
 - [20] F. Chen, G. L. Klimchitskaya, V. M. Mostepanenko, and U. Mohideen, Control of the Casimir force by the modification of dielectric properties with light, *Phys. Rev. B* **76**, 035338 (2007).
 - [21] J. M. Obrecht, R. J. Wild, M. Antezza, L. P. Pitaevskii, S. Stringari, and E. A. Cornell, Measurement of the temperature dependence of the Casimir-Polder force, *Phys. Rev. Lett.* **98**, 063201 (2007).
 - [22] G. L. Klimchitskaya and V. M. Mostepanenko, Conductivity of dielectric and thermal atom-wall interaction, *J. Phys. A: Math. Theor.* **41**, 312002 (2008).
 - [23] B. Geyer, G. L. Klimchitskaya, and V. M. Mostepanenko, Thermal quantum field theory and the Casimir interaction between dielectrics, *Phys. Rev. D* **72**, 085009 (2005).
 - [24] B. Geyer, G. L. Klimchitskaya, and V. M. Mostepanenko, Analytic approach to the thermal Casimir force between metal and dielectric, *Ann. Phys. (N.Y.)* **323**, 291 (2008).
 - [25] G. L. Klimchitskaya, U. Mohideen, and V. M. Mostepanenko, Casimir-Polder force between an atom and a dielectric plate: Thermodynamics and experiment, *J. Phys. A: Math. Theor.* **41**, 432001 (2008).
 - [26] G. L. Klimchitskaya, U. Mohideen, and V. M. Mostepanenko, The Casimir force between real materials: Experiment and theory, *Rev. Mod. Phys.* **81**, 1827 (2009).
 - [27] C. N. Li, A. B. Djurišić, C. Y. Kwong, P. T. Lai, W. K. Chan, and S. Y. Liu, Indium tin oxide surface treatments for improvement of organic light-emitting diode performance, *Appl. Phys. A* **80**, 301 (2005).
 - [28] J. R. Vig, UV/ozone cleaning of surfaces, *J. Vac. Sci. Technol. A* **3**, 1027 (1985).
 - [29] June Xu, G. L. Klimchitskaya, V. M. Mostepanenko, and U. Mohideen, Reducing detrimental electrostatic effect in Casimir-force measurements and Casimir-force-based microdevices, *Phys. Rev. A* **97**, 032501 (2018).
 - [30] G. Gómez-Santos, Thermal van der Waals interaction between graphene layers, *Phys. Rev. B* **80**, 245424 (2009).

- [31] D. Drosdoff and L. M. Woods, Casimir forces and graphene sheets, *Phys. Rev. B* **82**, 155459 (2010).
- [32] Bo E. Sernelius, Retarded interactions in graphene systems, *Phys. Rev. B* **85**, 195427 (2012).
- [33] A. D. Phan, N. A. Viet, N. A. Poklonski, L. M. Woods, and C. H. Le, Interaction of a graphene sheet with a ferromagnetic metal plate, *Phys. Rev. B* **86**, 155419 (2012).
- [34] N. Knusnutdinov, R. Kashapov, and L. M. Woods, Casimir-Polder effect for a stack of conductive planes, *Phys. Rev. A* **94**, 012513 (2016).
- [35] I. V. Fialkovsky, V. N. Marachevsky, and D. V. Vassilevich, Finite-temperature Casimir effect for graphene, *Phys. Rev. B* **84**, 035446 (2011).
- [36] M. Bordag, G. L. Klimchitskaya, and V. M. Mostepanenko, Thermal Casimir effect in the interaction of graphene with dielectrics and metals, *Phys. Rev. B* **86**, 165429 (2012).
- [37] M. Chaichian, G. L. Klimchitskaya, V. M. Mostepanenko, and A. Tureanu, Thermal Casimir-Polder interaction of different atoms with graphene, *Phys. Rev. A* **86**, 012515 (2012).
- [38] G. L. Klimchitskaya and V. M. Mostepanenko, Van der Waals and Casimir interactions between two graphene sheets, *Phys. Rev. B* **87**, 075439 (2013).
- [39] M. Bordag, G. L. Klimchitskaya, V. M. Mostepanenko, and V. M. Petrov, Quantum field theoretical description for the reflectivity of graphene, *Phys. Rev. D* **91**, 045037 (2015); **93**, 089907(E) (2016).
- [40] G. L. Klimchitskaya and V. M. Mostepanenko, Origin of large thermal effect in the Casimir interaction between two graphene sheets, *Phys. Rev. B* **91**, 174501 (2015).
- [41] M. Bordag, I. Fialkovskiy, and D. Vassilevich, Enhanced Casimir effect for doped graphene, *Phys. Rev. B* **93**, 075414 (2016); **95**, 119905(E) (2017).
- [42] G. Bimonte, G. L. Klimchitskaya, and V. M. Mostepanenko, Thermal effect in the Casimir force for graphene and graphene-coated substrates: Impact of nonzero mass gap and chemical potential, *Phys. Rev. B* **96**, 115430 (2017).
- [43] C. Henkel, G. L. Klimchitskaya, and V. M. Mostepanenko, Influence of chemical potential on the Casimir-Polder interaction between an atom and gapped graphene or graphene-coated substrate, *Phys. Rev. A* **97**, 032504 (2018).
- [44] G. L. Klimchitskaya, U. Mohideen, and V. M. Mostepanenko, Theory of the Casimir interaction for graphene-coated substrates using the polarization tensor and comparison with experiment, *Phys. Rev. B* **89**, 115419 (2014).

- [45] A. A. Banishev, H. Wen, J. Xu, R. K. Kawakami, G. L. Klimchitskaya, V. M. Mostepanenko, and U. Mohideen, Measuring the Casimir force gradient from graphene on a SiO₂ substrate, *Phys. Rev. B* **87**, 205433 (2013).
- [46] G. L. Klimchitskaya and V. M. Mostepanenko, Reflectivity properties of graphene with nonzero mass-gap parameter, *Phys. Rev. A* **93**, 052106 (2016).
- [47] G. Bimonte, T. Emig, R. L. Jaffe, and M. Kardar, Casimir forces beyond the proximity force approximation, *Europhys. Lett.* **97**, 50001 (2012).
- [48] G. Bimonte, T. Emig, and M. Kardar, Material dependence of Casimir forces: Gradient expansion beyond proximity, *Appl. Phys. Lett.* **100**, 074110 (2012).
- [49] L. P. Teo, Material dependence of Casimir interaction between a sphere and a plate: First analytic correction beyond proximity force approximation, *Phys. Rev. D* **88**, 045019 (2013).
- [50] G. Bimonte, Going beyond PFA: A precise formula for sphere-plate Casimir force, *Europhys. Lett.* **118**, 20002 (2017).
- [51] A. H. Castro Neto, F. Guinea, N. M. R. Peres, K. S. Novoselov, and A. K. Geim, The electronic properties of graphene, *Rev. Mod. Phys.* **81**, 109 (2009).
- [52] P. K. Pyatkovsky, Dynamical polarization, screening, and plasmons in gapped graphene, *J. Phys.: Condens. Matter* **21**, 025506 (2009).
- [53] V. P. Gusynin, S. G. Sharapov, and J. P. Carbotte, On the universal ac optical background in graphene, *New J. Phys. B* **11**, 095013 (2009).
- [54] L. A. Falkovsky, Optical properties of graphene, *J. Phys.: Conf. Series* **129**, 012004 (2008).
- [55] *Handbook of Optical Constants of Solids*, ed. E. D. Palik (Academic, New York, 1985).
- [56] L. Bergström, Hamaker constants of inorganic materials, *Adv. Colloid Interface Sci.* **70**, 125 (1997).
- [57] C.-C. Chang, A. A. Banishev, R. Castillo-Garza, G. L. Klimchitskaya, V. M. Mostepanenko, and U. Mohideen, Gradient of the Casimir force between Au surfaces of a sphere and a plate measured using an atomic force microscope in a frequency-shift technique, *Phys. Rev. B* **85**, 165443 (2012).

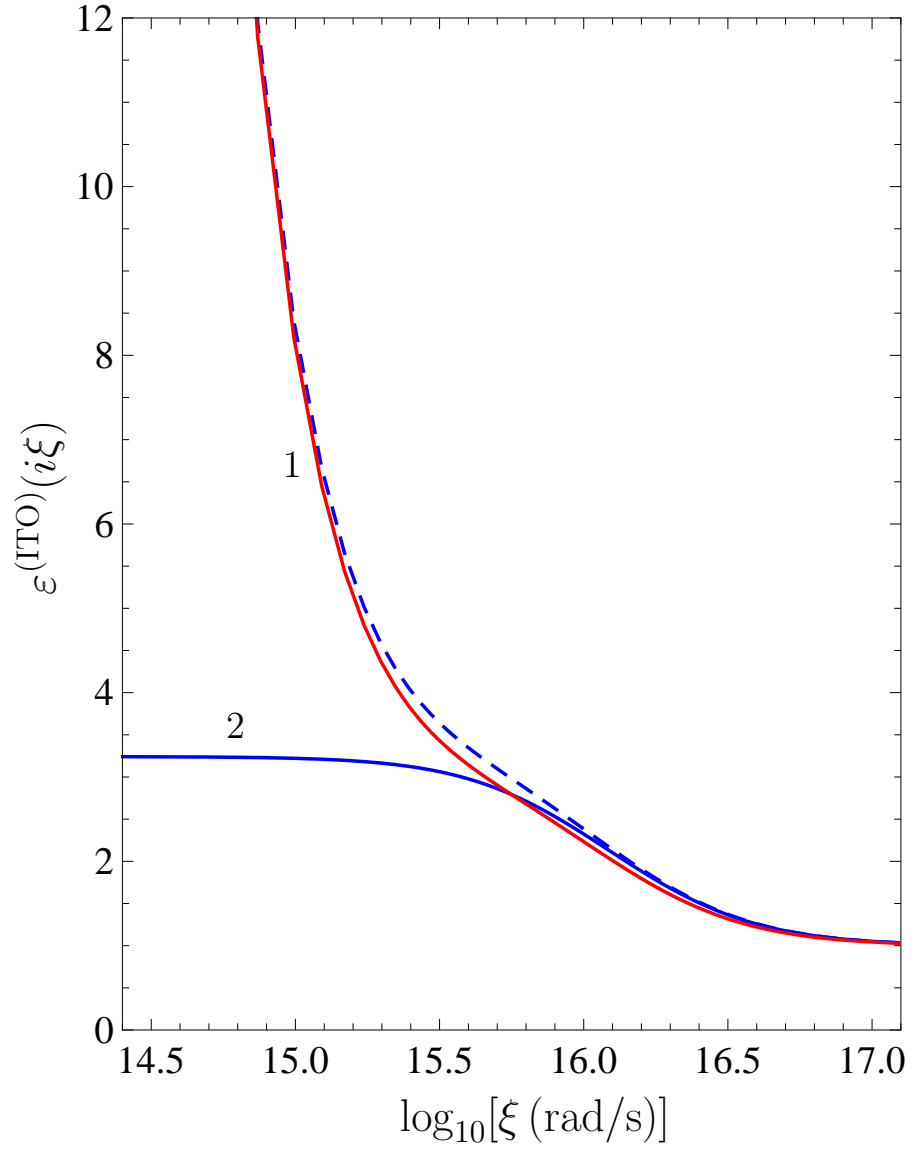


FIG. 1: The dielectric permittivity of an ITO film as a function of the imaginary frequency before the UV treatment with account of free charge carriers (the solid line 1) and after the UV treatment without account (the solid line 2) and with account (the dashed line) of free charge carriers.

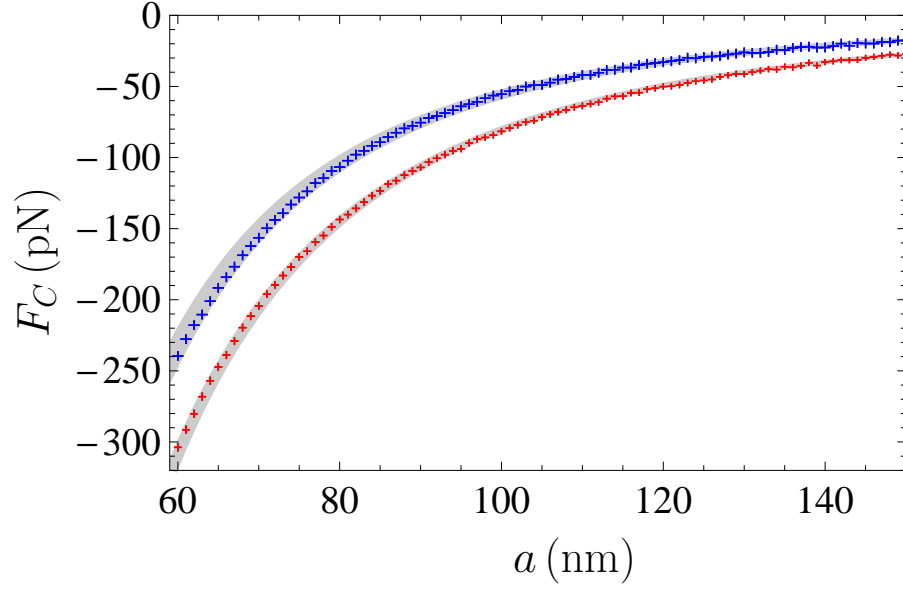


FIG. 2: The bottom and top bands show the Casimir forces between an Au sphere and an ITO film deposited on a quartz substrate calculated for the untreated and UV-treated films, respectively, at $T = 300$ K as functions of separation. The mean measured Casimir forces are indicated as functions of separation by the bottom and top sets of crosses for the untreated and UV-treated films, respectively.

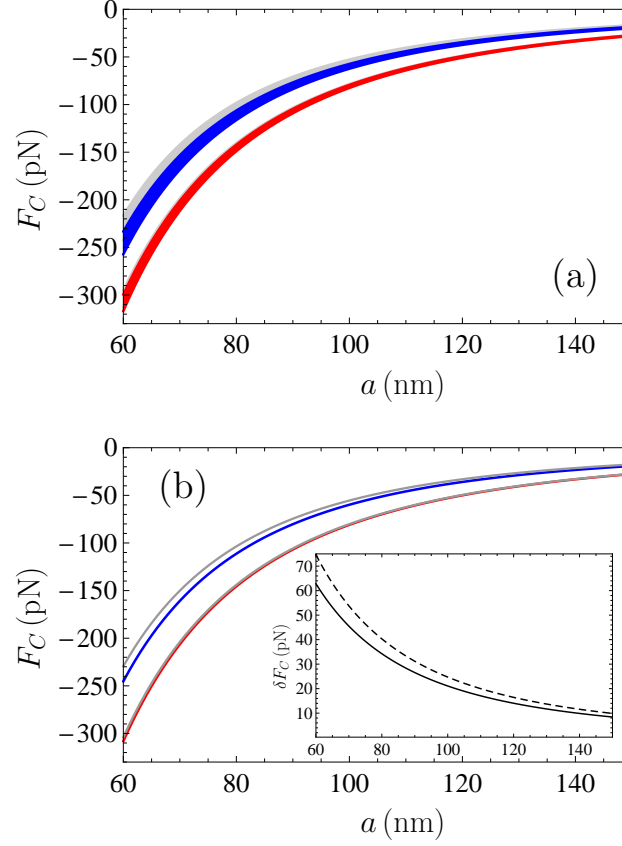


FIG. 3: (a) The bottom and top dark bands show the Casimir forces between an Au sphere and a graphene sheet on top of ITO film deposited on a quartz substrate calculated for the untreated and UV-treated films, respectively, at $T = 300$ K as functions of separation. The gray bands demonstrate similar results in the absence of a graphene sheet. (b) The mean lines of the above bands (see text for further discussion). In an inset the differences between the dark lines (the UV-treated and untreated ITO films coated with graphene) and between the gray lines (the uncoated UV-treated and untreated ITO films) are shown by the solid and dashed curves, respectively.

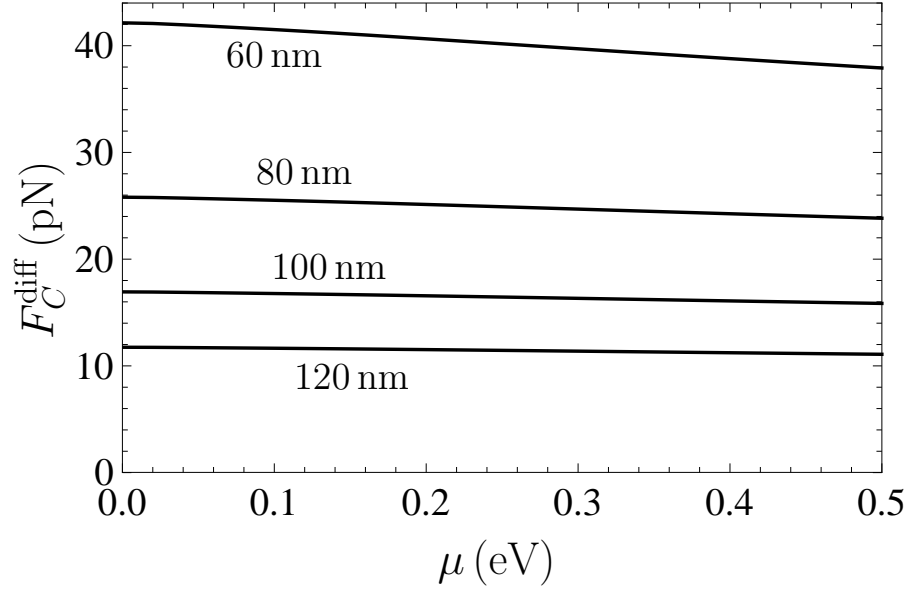


FIG. 4: The four lines from top to bottom show the minimum differences in the Casimir forces between an Au sphere and the UV-treated and untreated graphene-coated ITO samples calculated at $T = 300$ K at separations $a = 60, 80, 100$, and 120 nm, respectively, as functions of the chemical potential.

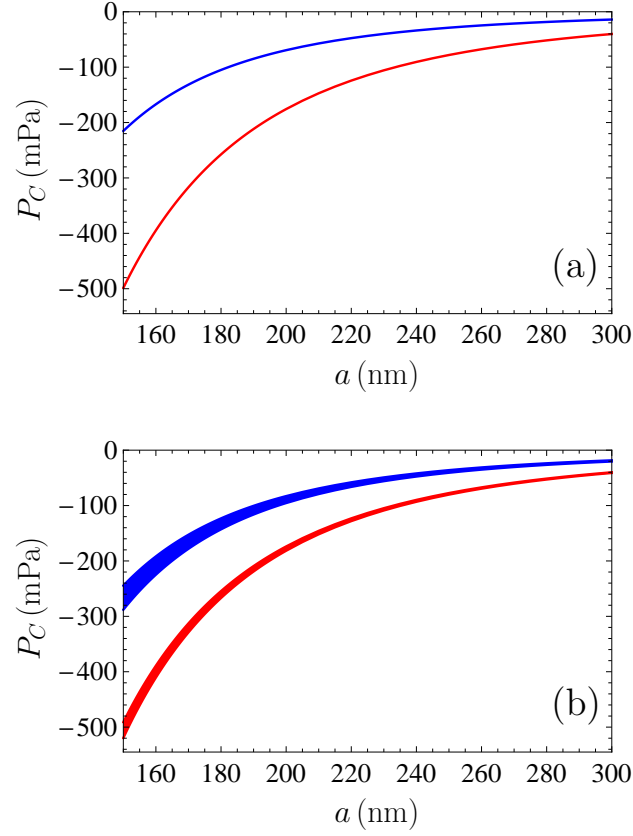


FIG. 5: (a) The mean values of the Casimir pressure between two plates consisting of ITO films deposited on quartz substrates are shown by the bottom and top lines computed for the untreated and UV-treated films, respectively, at $T = 300$ K as functions of separation. (b) The bottom and top bands show the Casimir pressure in the same conditions, but for the ITO films coated with additional graphene layers.

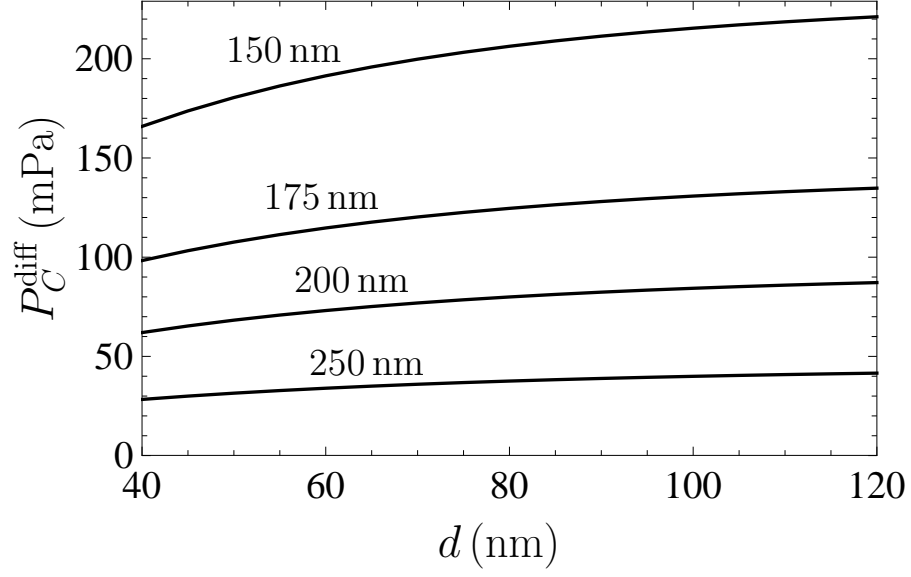


FIG. 6: The four lines from top to bottom show the minimum differences in the Casimir pressures between the UV-treated and untreated graphene-coated ITO samples calculated at $T = 300$ K at separations $a = 150, 175, 200$, and 250 nm, respectively, as functions of the thickness of ITO film.